How the site degree influences quantum probability on inhomogeneous substrates

A. M. C. Souza,[1] R. F. S. Andrade,[2] N. A. M. Araújo,[3,4] A. Vezzani,[5,6] and H. J. Herrmann[7,8]
[1]*Departamento de Física, Universidade Federal de Sergipe, 49100-000 Sao Cristovao, Brazil*
[2]*Instituto de Física, Universidade Federal da Bahia, 40210-210 Salvador, Brazil*
[3]*Departamento de Física, Faculdade de Ciências, Universidade de Lisboa, P-1749-016 Lisboa, Portugal*
[4]*Centro de Física Teórica e Computacional, Universidade de Lisboa, P-1749-003 Lisboa, Portugal*
[5]*IMEM-CNR, Parco Area delle Scienze, 37/A-43124 Parma, Italy*
[6]*Dipartimento di Scienze Matematiche, Fisiche e Informatiche, Università di Parma, via G.P. Usberti, 7/A-43124 Parma, Italy*
[7]*Computational Physics, IfB, ETH-Hönggerberg, Schafmattstrasse 6, 8093 Zürich, Switzerland*
[8]*Departamento de Física, Universidade Federal do Ceará, Campus do Pici, 60455-760 Fortaleza, Brazil*
(Received 22 May 2016; revised manuscript received 5 February 2017; published 18 April 2017)

We investigate the effect of the node degree and energy E on the electronic wave function for regular and irregular structures, namely, regular lattices, disordered percolation clusters, and complex networks. We evaluate the dependency of the quantum probability for each site on its degree. For a class of biregular structures formed by two disjoint subsets of sites sharing the same degree, the probability $P_k(E)$ of finding the electron on any site with k neighbors is independent of $E \neq 0$, a consequence of an exact analytical result that we prove for any bipartite lattice. For more general nonbipartite structures, $P_k(E)$ may depend on E as illustrated by an exact evaluation of a one-dimensional semiregular lattice: $P_k(E)$ is large for small values of E when k is also small, and its maximum values shift towards large values of $|E|$ with increasing k. Numerical evaluations of $P_k(E)$ for two different types of percolation clusters and the Apollonian network suggest that this observed feature might be generally valid.

DOI: 10.1103/PhysRevE.95.042130

I. INTRODUCTION

Electronic conduction is one of the most important properties of a solid. It depends essentially on the localized or delocalized character of the electronic wave function, which is related to the intrinsic properties of the atoms in the material and its crystalline structure. As is well known, the presence of disorder changes the extended character of the electronic states in periodic lattices, as established by Bloch's theorem [1]. The introduction of disorder (substitutional, vacancies, etc.) is the main mechanism controlling the Anderson transition [2]. Since disorder may emerge in many ways, different disorder types introduced on regular lattices produce different kinds of localized states [3].

In the case of substitutional disorder, a large number of results obtained on different systems indicates that the wave function has a strong tendency to be localized on the sites occupied by defects having a number of connections that significantly differs from the lattice average coordination [4–6]. The way this general property is manifested still depends largely on the detailed substitutions, as well as on the energy of the eigenstates. Thus, many issues remain open in understanding how the lattice structure [7], disorder [8], and eigenstate energy favor the wave function localization on particular sets of sites, and on the possibility of controlling the wave function localization [9–11],

Usually, the investigation of the effect of disorder on localization of a given system is targeted at the construction of the phase diagram in terms of the energy and a disorder control parameter, where the transition from the extended to the localized states can be clearly identified. Several global properties characterizing extended and localized states can also be obtained as a function of the quoted parameters.

In this paper, we focus our investigation on the relation between the degree of a given site in an inhomogeneous structure and the amplitude of the wave function in its neighborhood. We go beyond the knowledge that eigenstates with small values of E are likely to have large amplitudes for small values of k (particularly in the case of dangling bonds), and make a comprehensive investigation of the properties of $P_k(E)$, the probability of finding the electron in a given node (or site) of degree k, as a function of the energy E. We first consider the simple biregular lattices for which an exact theorem can be proven, indicating that $P_k(E)$ does not depend on E. Next, we consider a semiregular chain with nodes with degree 1 and 4 [12], for which the analytic evaluation of $P_k(E)$ uncovers a specific kind of dependency on E of small and large values of k. Particularly, we illustrate how its maxima move from the sites of small to large k when the value of $|E|$ increases. Further, we obtain numerical results for two kinds of inhomogeneous systems: (i) percolation clusters obtained according to the rules of usual bond percolation [13,14] and Gaussian percolation [15] and (ii) the Apollonian network (AN) [16]. This choice is justified by the fact that they display distinct and complementary features, namely, (i) randomly disordered, but with a relative small range of node degrees (1–4), and (ii) inhomogeneous and deterministic, but with a wide range of values of node degrees. For the Gaussian percolation cluster, we also present a more detailed, local analysis, by identifying how different sites with the same k contribute to $P_k(E)$.

Regarding the numerical investigation, we consider percolation clusters of two kinds on the square lattice of side L, subject to periodic boundary conditions, with $N = L \times L$ sites and N_b connections, $p = N_b/2N$ indicating the probability of a having a bond between nearest-neighbor sites. The models differ by the algorithm used to select bonds and, for the

same value of p, the number of sites with k neighbors, with $k \in [0,4]$, may be different. We consider values of p close to and above the percolation threshold p_c. We consider the percolation cluster which is a fractal of fractal dimension 91/48. According to current investigations, all wave functions at $p \gtrsim p_c$ are localized. The Apollonian network is characterized by a scale-free distribution of node degree and, as a consequence, the degree (number of connections) of a site varies in a wide interval. For this network, previous studies have indicated the presence of extended and localized states [17]. Finally, inhomogeneous chains are used to obtain exact results that help the discussion of more complex structures. The results for the local probability distribution as a function of the degree hint at further steps towards controlling wave localization at a given site on the percolation cluster.

The rest of this paper is organized as follows: In Sec. II, we present the electronic and two percolation models used to model a disordered system, and introduce two measures to characterize the electronic localization. Section III discusses exact results for semiregular lattices, which provide a useful comparison for the analysis that is presented for complex networks in Sec. IV and disordered systems in Sec. V. Finally, Sec. IV closes the paper with some final remarks on how the obtained results can be extended to more complex geometries.

II. THE MODEL

The simplest model for electric conduction is based on a one-particle tight-binding Hamiltonian. If we consider an ordered system on a periodic Bravais lattice, the electron interacts with the atom at any lattice site **r** with on-site energy $\epsilon_{\vec{r}}$, but it only jumps from $\vec{r}$ to site $\vec{r'}$ with a hopping probability $V_{\vec{r},\vec{r'}} = V_{\vec{r'},\vec{r}}$ if the two sites satisfy some conditions. Usually, it is assumed that $V_{\vec{r},\vec{r'}} = 0$ unless $\vec{r}$ and $\vec{r'}$ are next neighbors and, if this is satisfied, $V_{\vec{r},\vec{r'}}$ is a constant independent of the pair of interacting sites. This is justified by the fact that the hopping term results from the overlap integral of two one-particle wave functions localized on neighboring sites mediated by an interaction potential. Moreover, if there is no inhomogeneity in the on-site binding energy $\epsilon_{\vec{r}}$, as we consider hereafter, it is conventional to set $\epsilon_{\vec{r}} \equiv 0, \forall \vec{r}$. Therefore, the system Hamiltonian is written as

$$\mathbf{H} = \sum_{(\vec{r},\vec{r'})} V_{\vec{r},\vec{r'}} |\vec{r}\rangle\langle\vec{r'}|. \tag{1}$$

The eigenstates of **H** corresponding to eigenvalue $E(\vec{\kappa})$ are denoted by $|\psi_E\rangle$, so that the solutions of the Schrödinger equation are the wave function $\psi_E(\vec{r}) = \langle\vec{r}|\psi_E\rangle$, where $\vec{\kappa}$ denotes the wave vector so that $E = E(\vec{\kappa})$.

The Hamiltonian (A3) can also be extended to describe disordered systems on percolating clusters, or on inhomogeneous substrates like the AN obtained through the recursive application of a geometrical procedure leading to a series of network generations labeled by g.

In all cases we consider here, the local energy parameter $\epsilon_{\vec{r}}$ is assumed to be constant and, without loss of generality, is set to zero, which allows us to concentrate on the effect of topological disorder. For the percolation clusters, we consider $V_{\vec{r},\vec{r'}} = V_0$ or 0, according to whether a bond between the sites $\vec{r}$ and $\vec{r'}$ is present or not. For inhomogeneous substrates, $V_{\vec{r},\vec{r'}} = V_0 = 1$ or 0 according to whether the corresponding sites are connected or not. For the AN, the tight-binding model is described by a sequence of Hamiltonian operators $\mathbf{H_g}$, which account for all interactions between the sites introduced until the generation g. Details of this kind of investigation can be found in Refs. [17,18], where an investigation of the properties of the eigenstates for successive generations of the Apollonian network has been carried out. The site labeling used herein has been introduced in Ref. [17].

Like in the classical percolation transition, the probability p is also the control parameter for the the localized-extended transition, which some times is referred to as quantum percolation [19,20]. A quantum percolation threshold p_q can be defined as the smallest value of p for which there exists an eigenvalue E of the Schrödinger equation such that $|\psi_E\rangle$ is an extended eigenstate in the sense that it is not possible to find any finite region such that the sum of $|\psi_E(\vec{r})|^2$ over all sites outside this region is smaller than any arbitrarily chosen positive number. The critical values p_q for the quantum problems are usually larger than the corresponding percolation transition values p_c. For instance, for the square lattice, the bond percolation transition occurs at $p_c = 0.5$. However, great controversy persists about the precise value of the quantum percolation threshold [21–27].

In the usual random percolation problem, an empty connection is randomly chosen to be occupied in a sequential order. To obtain percolation clusters according to the Gaussian model [15], one starts with a regular lattice without bonds. The original bonds of the corresponding Bravais lattice are selected uniformly at random and added to the lattice with probability q, given by

$$q = \min\left\{1, \exp\left[-\alpha\left(\frac{s-\bar{s}}{\bar{s}}\right)^2\right]\right\}, \tag{2}$$

where s is the size of the cluster of connected sites that will be formed if the bond is added to the system and $\bar{s}$ is the average cluster size. Differently from the usual percolation clusters, the clusters that emerge at p_c with the Gaussian rule are compact with a fractal perimeter.

To characterize the localization of the time independent wave function, we analyze the participation ratio (ξ) associated to the eigenvectors of the eigenvalues E, which has been successfully used to characterize the localization of the wave function for a large variety of systems. In the case of absence of degenerate energy eigenstates, ξ is generally defined as [17]

$$\xi(E) = \frac{1}{\sum_{\vec{r}} |\psi_E(\vec{r})|^4}, \tag{3}$$

where $\psi_E(\vec{r})$ is the wave function amplitude on site $\vec{r}$. A localized eigenstate is characterized by $\xi(E)/N \to 0$ in the limit $N \to \infty$, but this ratio converges to a finite value if the state is extended. In the case of energy degeneracy, e.g., with G eigenstates of same energy E, Eq. (A5) can be replaced by

$$\xi(E) = \frac{1}{\sum_{\vec{r}} \left(\frac{1}{G}\sum_{j=1}^{G} |\psi_{E,j}(\vec{r})|^2\right)^2}. \tag{4}$$

Along the same line, to account for any energy degeneracy, we characterize the k-dependent probability of finding the particle at a site of degree $\bar{k}$, by

$$P_{\bar{k}}(E) = \sum_{\vec{r}} \frac{1}{G} \sum_{j=1}^{G} |\psi_{E,j}(\vec{r})|^2 \delta_{k(\vec{r}),\bar{k}}, \tag{5}$$

with the same normalization condition $\sum_k P_k(E) = 1$.

Our investigation is based on the systematic evaluation of the relation between $\psi_E(\vec{r})$ and the site degree $k(\vec{r})$, from which the distribution $P_k(E)$ can be evaluated. As we will show in the next sections, the definition in Eq. (5) provides useful insights on the distribution probability of finding the particle on sites with different values of k as a function of the energy.

In the case of percolation clusters, we restrict our analysis to those clusters evaluated at $p \gtrsim p_c$ as well for the usual random occupation algorithm as for the Gaussian model of discontinuous percolation. In the case of the Apollonian network, we consider the situation in which all connections defined by the construction procedure correspond to a single value of the hopping integral.

III. SEMIREGULAR AND BIPARTITE NETWORKS

Before presenting the results of our simulations, let us briefly discuss some aspects of wave function localization in some simple structures, which help understanding the behavior observed for more complex geometrical arrangements. For the sake of clarity in the discussion of our results, let us define the terms used in this paper, starting with the mathematical definition of a graph or general network (see, e.g., [28–30]). A graph $G(V,E)$ is a set V of vertices (or nodes, or sites) i connected pairwise by a set E of undirected edges (or connections) (i,j). In particular the quantum problem defined by Hamiltonian (1) is exactly the spectrum of the adjacency matrix of the graph [31,32]. For a precise characterization of the spectral graph problem we address in this paper, we note the following:

(i) A *lattice* is a (periodic) network that remains invariant under a certain set of translations in space.

(ii) In a *regular* network, all nodes have the same degree.

(iii) In a *semiregular* network, all nodes can be cast into two sets (say S_1 and S_2), so that all nodes in S_1 (S_2) have degree k_1 (k_2).

(iv) Networks are *bipartite* when the nodes can be split into two disjoint sets, in such a way that any site in the set S_1 (S_2) is only directly connected to sites in set S_2 (S_1).

Note that a given structure can satisfy one or more of the above criteria. A trivial example of a bipartite lattice is the square lattice that can be split into two sublattices with the above property. It is easy to observe that the bipartite concept can be easily extended to include a larger number of partitions (e.g., the face centered cubic lattice is quadripartite). Independently of being or not being a lattice, it is possible to cast the semiregular networks into two different classes according to the following criterion: we call biregular or semiregular of class A those semiregular networks where the sets S_1 and S_2, characterized by degree k_1 and k_2, respectively, also define a bipartition of the graph, i.e., the links connect only sites belonging to S_1 with sites belonging to S_2. Semiregular but nonbiregular networks belong to class B. Class A satisfies the following condition: the product of the site degree of each set by the number of sites in this set is the same for the two sets. On the other hand, semiregular networks in class B do not satisfy this condition. For instance, the square lattice belongs to class A.

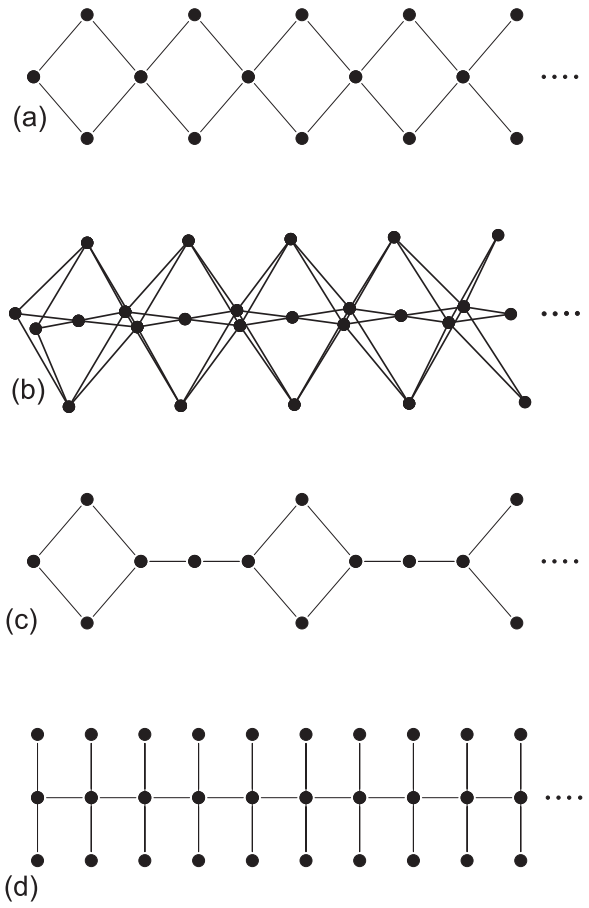

FIG. 1. Examples of biregular (a–c) and semiregular (d) decorated linear chains.

An important analytical result can be derived for some biregular lattices of class A: the probability $P_k(E)$ of finding an electron on each of the two sets of sites is independent of the energy $E \neq 0$ (see the Appendix, where we provide a very general proof of this property). Regarding semiregular structures of class B (nonbipartite), it is easy to find counterexamples showing that the above stated result does not hold. As our results show, the exact results for this very general topological classification can be used to explain specific wave function properties for tight-binding models built on regular Euclidian lattices, percolation clusters, and complex networks.

For illustrative purposes, we first apply this approach to one-dimensional decorated chains (lattices) in classes A and B, which have been extensively used to model polymeric chains [33,34]. This provides very simple exact results for the dependency between $\psi_E(\vec{r})$ and $P_k(E)$, supporting our results for the Apollonian network and percolation clusters. Figures 1(a)–1(c) (see Ref. [12]) present examples of lattices of class A. Indeed, if in Fig. 1(a) the lattice has N sites, the set S_1 comprises $2N/3$ sites with degree $k = 2$, while the

remaining $N/3$ sites with $k = 4$ belong to S_2. In Fig. 1(b), the set S_1 has $3N/5$ sites, with degree $k = 4$, while the set S_2 has $2N/5$ sites with $k = 6$. In Fig. 1(c), S_1 has $3N/5$ sites with degree $k = 2$, and S_2 has $2N/5$ sites with $k = 3$. Finally, the lattice in Fig. 1(d) belongs to class B: it is semiregular and bipartite, but the set S_1 with $N/3$ sites with $k = 4$, and the set S_2 of $2N/3$ sites with $k = 1$, do not define a bipartition of the lattice.

All eigenvalues and corresponding wave functions (eigenvectors) of the tight-binding Hamiltonian (A3) for each of the simple structures in Fig. 1 can be easily evaluated. Moreover, the periodicity of the structures assures that all wave functions have extended character. After briefly addressing the analytical result that is valid for the lattices in Figs. 1(a) and 1(b) (see the Appendix for the details of our results), let us consider the lattice in Fig. 1(d). For each value of the energy $E(\kappa)$ (here κ denotes the one-dimensional quantum wave vector) there exist two different expressions for the probability of finding the particle in a site of the set S_1 and S_2, respectively. It is straightforward to show that the probability $P_k(E)$ is given by

$$P_{k=1}(E) = \frac{2}{E^2+2}, \tag{6}$$

$$P_{k=4}(E) = \frac{E^2}{E^2+2}. \tag{7}$$

The above expressions are valid for any of the three possible solutions $E(\kappa)$ of the Schrödinger equation derived from the appropriate tight-binding Hamiltonian for the network. Each of the three families of solutions, given by $E(\kappa) = 0$, $E = E(\kappa) = \cos(\kappa) \pm \sqrt{\cos(\kappa)^2 + 2}$, accounts for one third of all possible quantum states. The above equations indicate that the amplitude of the wave function in a certain site depends on its degree. For instance, when $E = 0$, all degenerate states satisfy $P_{k=2}(E = 0) = 1$ and $P_{k=4}(E = 0) = 0$. For the other two energy bands, Fig. 2 shows that, when $|E|$ shifts from $\sqrt{3} - 1$ towards the band edges at $|E| = \sqrt{3} + 1$, $P_k(E)$ decreases (increases) for $k = 2$ ($k = 4$), as a function of $E(\kappa)$. We would like to note that this peculiar dependency of $P_k(E)$ on k and E is not limited to this simple semiregular, periodic, one-dimensional chain. Indeed, as will be illustrated in the next sections, it will recursively appear in our results for inhomogeneous substrates like the Apollonian network and the two types of percolation clusters. Thus, it is reasonable to admit that such a universal behavior must rely on a physical mechanism present in all systems, as we briefly discuss in the last section.

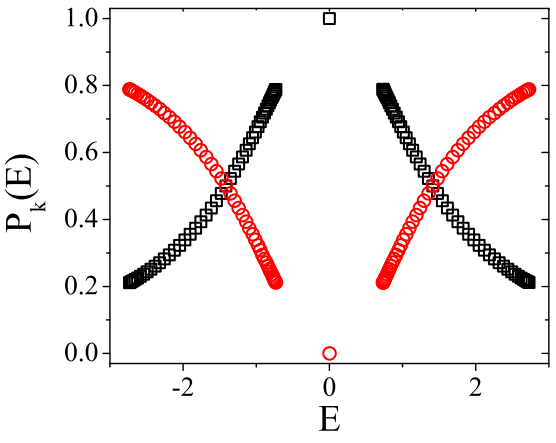

FIG. 2. Probability of finding the particle on the set of sites with different degree according to Eqs. (A6) ($k = 2$, squares) and (7) ($k = 4$ circles) as a function of the wave function energy.

To characterize the localization character of the wave function for $E(\kappa) \neq 0$, we evaluate $\xi(E)$ defined by Eq. (4). It is straightforward to obtain the expression

$$\xi(E) = \frac{N(E^2+2)^2}{3(E^4+2)}, \tag{8}$$

indicating that $\xi(E) \propto N$ for any energy. Moreover, sites with different values of k have nonzero square modulus of the wave function, which is also delocalized for the ordered structures in Fig. 1(d).

The numerical findings discussed in the next sections indicate a similar dependency of $P_k(E)$ with respect to both k and E for more complex systems; we would like to remark that general proofs for the validity of the above observations for any system with more than two types of sites are still required. Although they are surely beyond the scope of this paper, the above discussion sheds light on the interpretation of some of our results in the next section.

IV. $P_k(E)$ FOR THE APOLLONIAN NETWORK

Now let us discuss the dependency of the probability of site occupation $P_k(E)$ as a function of energy for a geometrical model where the site degree can take integer values in a much wider interval. Despite the fact that several geometrical sets may present this property, we concentrate our investigation on the tight-binding model on the AN. This model has been used in many studies as an example of a deterministic geometric structure that has many features of complex networks, such as scale free distribution of node degree, small world property, hierarchical structure, and so on [16]. Its origin is related to the Apollonian packing, which emerges as the solution to the space filling problem. The network can be constructed in a simple recursive way, by starting at generation $g = 0$ with an equilateral triangle. The construction step in the gth generation of the network consists in adding a node within each triangle of the previous generation, and connecting it to each of the triangle corners. For each value of g, $N(g) = (3^g + 5)/2$ and $B(g) = (3^{g+1} + 3)/2$ express, respectively, the number of nodes $N(g)$ and edges $B(g)$. Because of its simplicity and concomitant similarity to many random complex networks, most of its quantum energy spectrum features, eigenstate localization properties, and quantum walk dynamics have been described in detail in several works [17,18,35–37]. For instance [17], it is well known that the energy levels are discrete, and also that any eigenvalue that belongs to the energy spectrum having a particular value of g will also be present in the spectra of all $H_{g'}$ with $g' > g$. The energy levels are highly degenerated, and the degeneracy of a level introduced in the spectrum at a given value of g increases with the difference $g' - g$, for $g' > g$.

Because of the discrete nature of the spectrum, we cannot expect to have a smooth dependency of $P_k(E)$ on E. Nevertheless, it is possible to identify that the overall trend displayed in

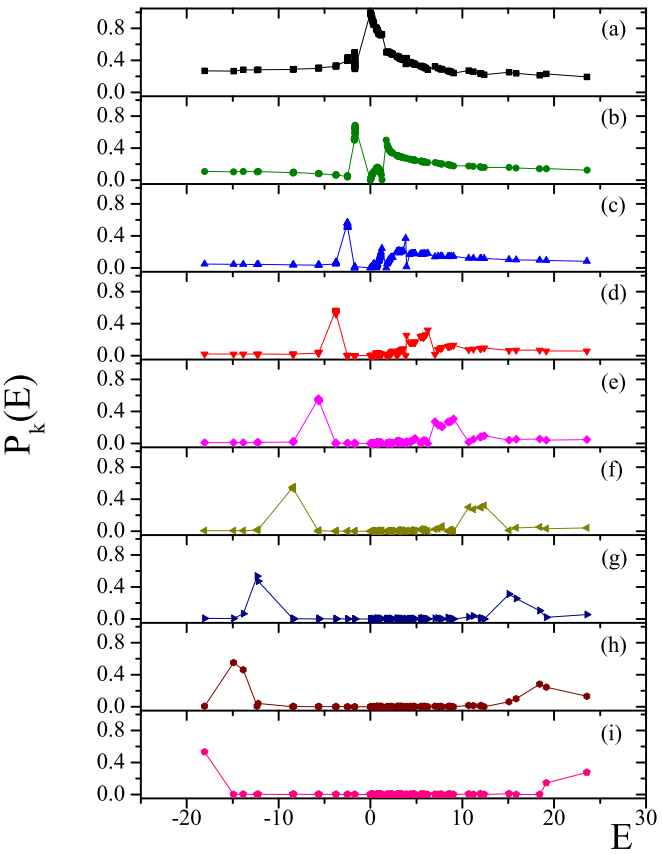

FIG. 3. Probability of finding the particle on the set of sites with different degree as a function of the wave function energy for the Apollonian network with $g = 8$. With exception of panel (h), for which $k = 257$, panels (a)–(g) and (i) correspond, respectively, to degrees $k = 3 \times 2^m$, with $m = 0,1,\ldots,7$.

Fig. 2 is reproduced in Fig. 3. For the sake of clarity, we show individual plots of $P_k(E)$ as a function of E for each possible value of k at $g = 8$, when the network comprises 3283 sites. We see that, for small wave vector k, $P_k(E)$ is characterized by large values at small energies $|E|$, while it becomes small for the levels at large $|E|$. The successive panels indicate that this pattern changes progressively for increasing values of k. Large values of $P_k(E)$ can be identified at larger and larger values of $|E|$. If we draw continuous peaks that are upper bounds to the allowed values of $P_k(E)$, we notice that the positions of these peaks are shifted to larger values of $|E|$ as k increases.

We recall that the number of sites with small (large) value of k is large (small). As $P_k(E)$ does not identify particular sites with degree k, it is natural that the plots of $P_k(E)$ are denser (less dense) for small (large) values of k. Finally, it is interesting to observe that, as g' increases, the probability of finding a particle at a particular site introduced in the network at generation $g < g'$ is shifted to larger values of $|E|$.

This example shows that it is possible to exert control over the location of the electron on sites with different degree k by an adequate choice of the wave function energy. This is particularly straightforward in the case of the Apollonian network because of the discrete character of its energy spectrum.

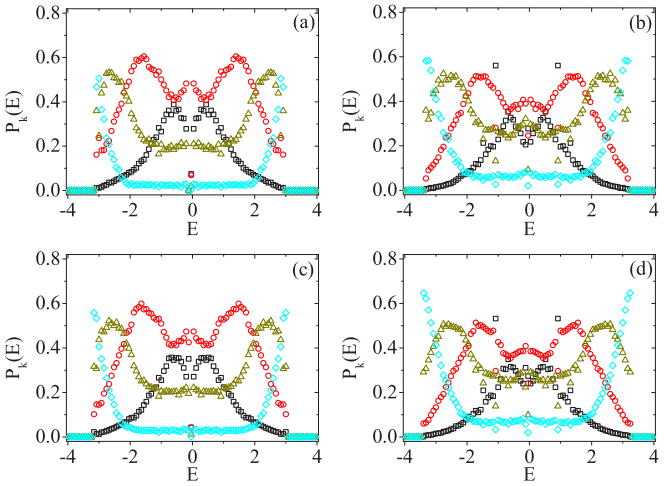

FIG. 4. Probability of finding the particle on sites with different degree as a function of the wave function energy for percolation clusters obtained by the Gaussian (a, c) and usual models (b, d) when $p = p_{c,G} = 0.56244$. The used samples correspond to $L = 32$ (a, b) and $L = 64$ (c, d). Black squares, red (dark gray) circles, dark yellow (gray) triangles, and cyan (light gray) diamonds indicate data points for node degree $k = 1,2,3,$ and 4, respectively.

V. THE SITE PROBABILITY DISTRIBUTION IN PERCOLATION CLUSTERS

In this section we discuss the probability $P_k(E)$ of finding the particle on a site of degree k, for both the Gaussian and usual random percolation models on the square lattice. Each plot with the results of our numerical simulations consists of four branches for $k = 1,2,3,4$. Differently from the previous deterministic situations, the results for each model represent averages over m independent samples, obtained according to the same random procedure, and for given values of L and p. As we show, depending on the value of these parameters, large fluctuations can still be noticed for $P_k(E)$.

The wave functions have been obtained by numerically evaluating all eigenvalues and eigenvectors of the Hamiltonian (A3). Figures 4 and 5 show the results for both usual and Gaussian models, for $N = 32^2$ and 64^2 and, respectively, bond inclusion probability $p = 0.56244$ and 0.8. The first value of p was chosen to correspond to the percolation threshold $p_{c,G}$ of the Gaussian model, which is larger than the critical probability $p_{c,U} = 0.5$ for the usual model. All results were obtained by averaging $P_k(E)$ over ten independently generated samples for each value of p.

The comparison of the figures clearly shows that, by decreasing the randomness in the location of bonds, which is achieved by increasing p in the interval $[0.5,1]$, the fluctuations of $P_k(E)$ with respect to E become largely damped. Next, we observe that $P_k(E)$ associated to each value of k depends on p through the number of sites within each subset. The visual comparison between the average location of points in the two figures indicates that the number of sites in S_4 has increased when p changes from 0.564 to 0.8, while the opposite is observed for the sets S_1 and S_2. The situation for S_3 is more complex: $P_{k=3}(E)$ increases in the central part of the spectrum, but remains roughly at the same height in the previous peaks

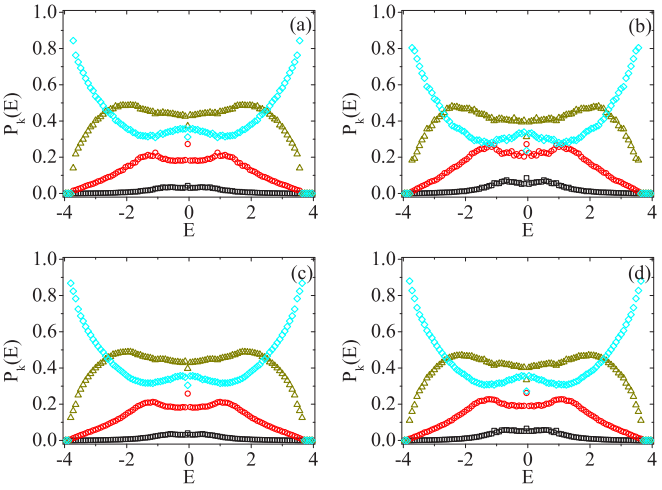

FIG. 5. Probability of finding the particle on sites with different degree as a function of the wave function energy for percolation clusters obtained by the Gaussian (a, c) and usual models (b, d) when $p = p_{c,G} = 0.8$. The used samples correspond to $L = 32$ (a, b) and $L = 64$ (c, d). Black squares, red (dark gray) circles, dark yellow (gray) triangles, and cyan (light gray) diamonds indicate data points for node degree $k = 1,2,3$, and 4, respectively.

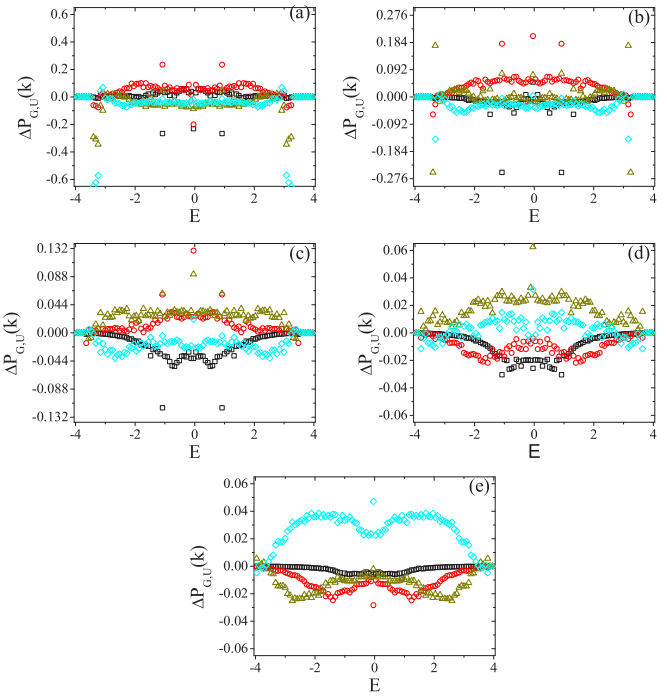

FIG. 6. Dependency of $\Delta P_{G,U}(k) = P_{k,G}(E) - P_{k,U}(E)$ as a function of E for decreasing probabilities $p = 0.56244, 0.6, 0.7, 0.8$, and 0.9, when $L = 64$. Since $\Delta P_{G,U}(k)$ decreases as p increases, the vertical axis is conveniently rescaled in each panel. For different k, the relative positions of $\Delta P_{G,U}(k)$ also change with p. Black squares, red (dark gray) circles, dark yellow (gray) triangles, and cyan (light gray) diamonds indicate data points for node degree $k = 1,2,3$, and 4, respectively.

situated at $E \simeq \pm 2.2$. The position for the curves for $L = 32$ and 64 is almost identical for the Gaussian model, but some differences still can be observed for the usual model. Here, the most important deviation occurs with the branch for $k = 2$.

The different dependency of $P_k(E)$ on E in both models, for $k = 3$ and 4, in Fig. 5 clearly recalls the behavior shown in Fig. 2: the probability for $k = 4$ sites is enhanced for energies close to the end of the spectrum, and depleted for the sites with $k = 3$. This effect can also be observed for the smaller value $p = 0.56244$, as well as for $k = 0, 1$, and 2: all of them decay to zero when $|E|$ increases much faster than the branches for larger values of k.

It is possible to identify several distinct features having the form of $P_k(E)$ for the two percolation models, which can be better visualized if we consider the differences between the results for the two percolation models for the same values of L and p. The results are illustrated in Fig. 6, where we show $\Delta P_{G,U}(k) = P_{k,G}(E) - P_{k,U}(E)$ as a function of E, for $L = 64$. The additional subscripts G and U identify the Gaussian and usual versions. Substantial differences appear at $p = 0.56244$, which gradually decrease when p increases. To make the differences visible, the vertical scales are gradually reduced, so that they differ by a factor 10 when we go from $p = 0.56244$ to 0.8. This is an expected dependency, once the percolation clusters generated by the two models attain their largest difference at $p_{c,G}$. Since both models converge to the complete lattice at $p = 1$, the differences in the percolation clusters and the localization properties disappear as p increases. However, the reduction in $\Delta P_{G,U}(k)$ is followed by several changes in the position of its k-dependent branches as p is increased. For $p = p_{c,G}$, the $k = 1$ and 2 branches are positive, while the others are negative. As p increases, the situation is reversed. The $k = 1$ and 2 branches become negative, while those for $k = 3$ and 4 increase. At $p = 0.9$, only the $k = 4$ branch is positive. This is a quite interesting behavior of the probability $P_k(E)$, revealing that the behavior of the wave function is quite sensitive to differences in the geometric structure of the system.

Once $P_k(E)$ results from the sum of the individual contributions of all sites of a given k, complementary information about the wave function distribution can be provided by $\Pi_k[\rho_E(\vec{r})]$, the distribution of site occupancy probability for each subset of sites with a given connectivity k, as a function of $\rho_E(\vec{r}) = |\psi_E(\vec{r})|^2 \delta_{k(\vec{r}),k}$. Because several quantum states are strongly localized and the value of $\rho_E(\vec{r})$ has a wide variability, it is more convenient to consider the dependency of $\Pi_k[\rho_E(\vec{r})]$ on $\log_{10}[\rho_E(\vec{r})]$ rather than on $\rho_E(\vec{r})$, as we have done. Figures 7 and 8 illustrate the behavior of $\Pi_k[\rho_E(\vec{r})]$ as a function of $\log_{10}[\rho_E(\vec{r})]$ for wave functions on Gaussian percolation clusters, with $L = 64$ and selected values of p, k, and E. To analyze these results, it is convenient to keep in mind the general trend of $P_k(E)$ to have larger values at the band edges for larger values of k, irrespective of the other variables. Thus, the distribution $\Pi_k[\rho_E(\vec{r})]$ reflects the fact that $\psi_E(\vec{r})$ depends on E, on p, and on the extended or localized character of the quantum state. The value of p interferes with the fraction of sites with different degree which, in turn, also influences the localization properties of $\psi_E(\vec{r})$. Figure 7 shows that, for $p = 0.8$, when there is no site with degree $k = 0$, $\Pi_k[\rho_E(\vec{r})]$ is peaked on values of $\rho \lesssim 10^{-4}$ at the band center ($E = -0.01$) as well as at intermediate $E = -1.50$ for all $k > 0$. Such a distribution hints towards a strongly delocalized character of

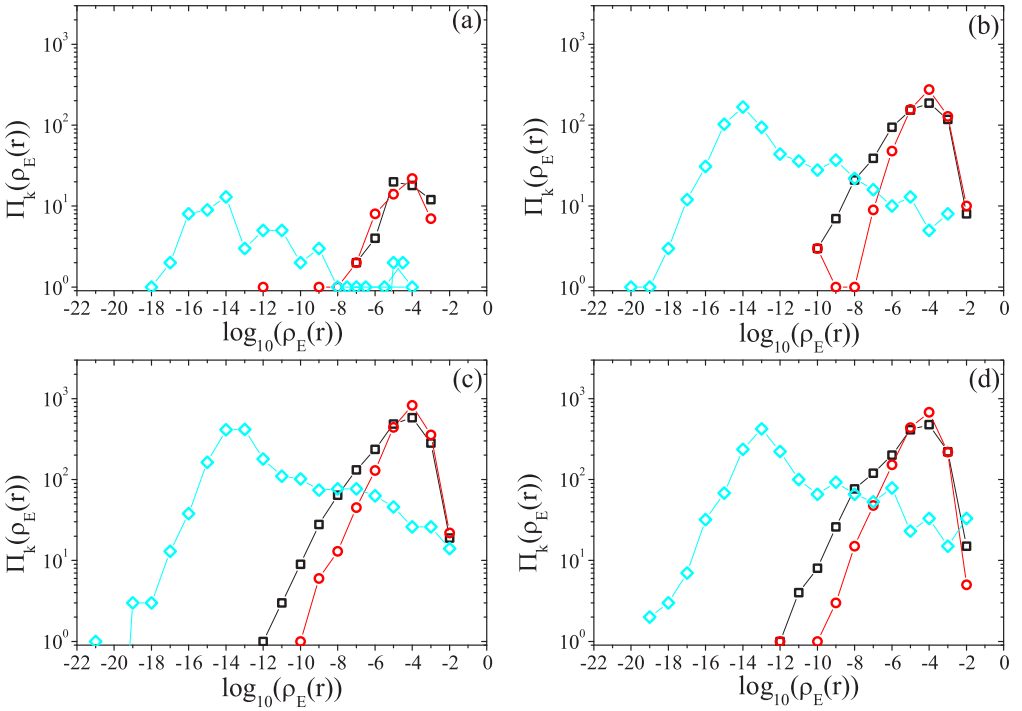

FIG. 7. Distribution of site occupancy probability $\Pi_k(\rho_E(\vec{r}))$ as a function of $\log_{10}[\rho_E(\vec{r})]$ for systems with $L = 64$. Points in panels (a)–(d) correspond, respectively, to number of sites with $k = 1$–4 in histograms with bin width 1, for $p = 0.8$. Black squares, red (dark gray) circles, and cyan (light gray) diamonds indicate data points for $E = -0.01$, -1.50, and -3.65, respectively.

ψ_E, with weak dependency on the degree of each site. This can be seen by comparing this distribution to the result obtained for a completely uniform wave function over all 4096 lattice sites. In such case, $\Pi_k[\rho_E(\vec{r})]$ corresponds to a single peak at $\rho = 2.44 \times 10^{-4}$. This contrasts with curves for the band edge energy $E = -3.65$, which are peaked at $\log_{10}(\rho) \sim -12$ and show a decreasing tail when ρ increases. Although this general behavior is independent of k, we notice that the curve for $k = 2$

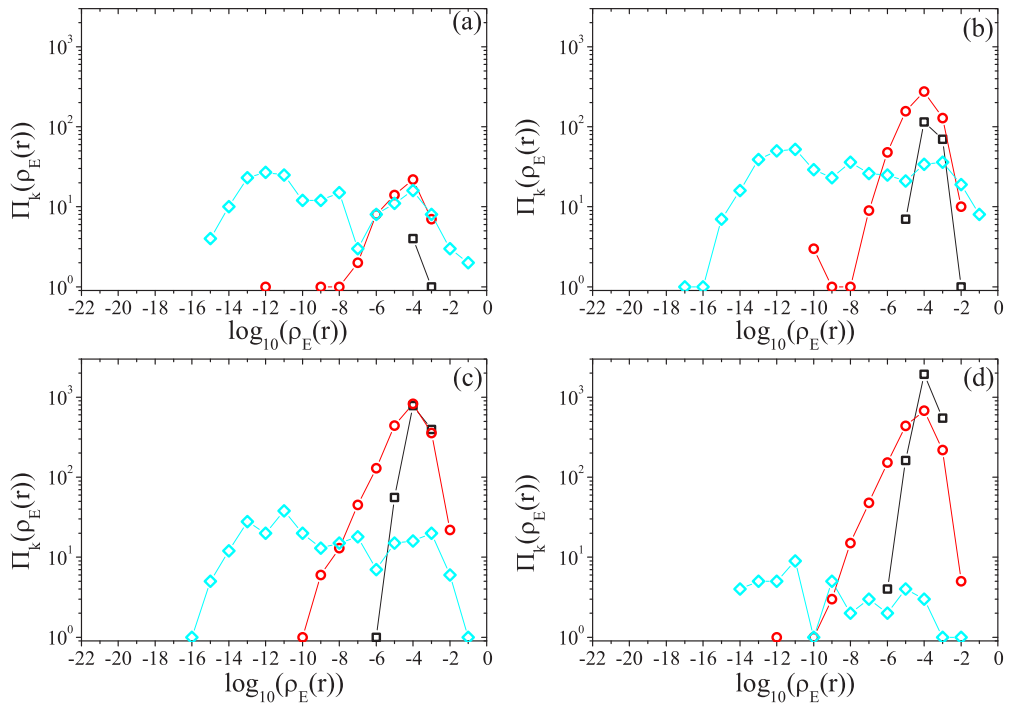

FIG. 8. Distribution of site occupancy probability $\Pi_k[\rho_E(\vec{r})]$ as a function of $\log_{10}[\rho_E(\vec{r})]$ for systems with $L = 64$. Points in panels (a)–(d) correspond, respectively, to number of sites with $k = 1$–4 in histograms with bin width 1, for $E \simeq -1.5$. Black squares, red (dark gray) circles, and cyan (light gray) diamonds indicate data points for $p = 0.9, 0.8$, and p_c, respectively.

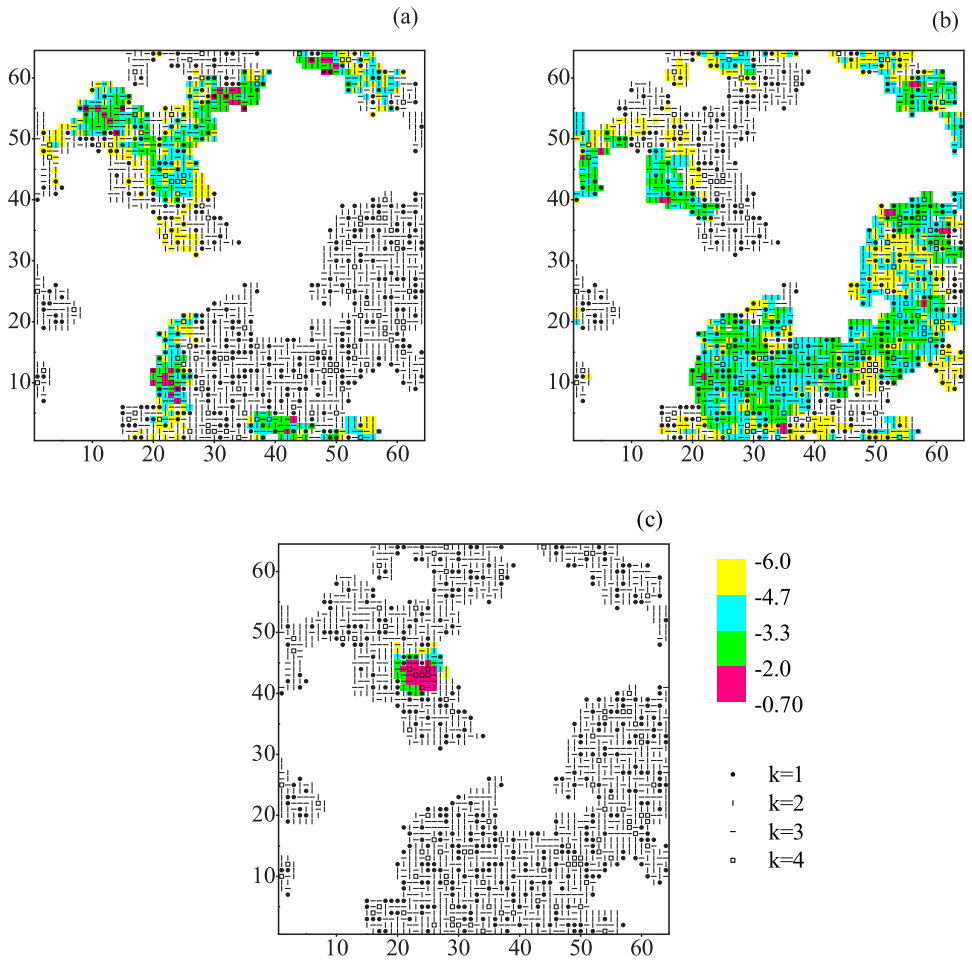

FIG. 9. Color plots of $\log_{10}[\rho_E(\vec{r})]$ as a function of position for a percolation cluster at $p = p_c$, for $E = -0.2$, -1.5, and -3.065, in panels (a)–(c). White region corresponds to sites with $k = 0$. Sites with $k = 1$–4 are indicated, respectively, by circles, vertical bars, horizontal bars, and open squares. Sites with $\log_{10}[\rho_E(\vec{r})] < -6$ remain white, otherwise they are shaded according to a color (gray tone) code for the following intervals: (i) yellow (very light gray), $[-6, -4.7)$; (ii) cyan (light gray), $[-4.7, -3.3)$; (iii) green (gray), $[-3.3, -2.0)$; and (iv) pink (dark gray), $[-2.0, -0.7]$. Only the state close to the band edge ($E = -3.065$) displays strong localization, with peaks centered on $k = 4$ sites. The less localized states with $E = -0.2$ and -1.5 are spread over sites with different values of k.

has a contribution for $\log_{10}(\rho) = -3$ while, for $k = 3$ and 4, important contributions from $\log(\rho) = -2$ are observed. Thus, ψ_E corresponds to a strongly localized state on a small set of sites, with the largest contributions coming from sites of large k. Figure 8 illustrates the behavior of $\Pi_k[\rho_E(\vec{r})]$ for one same E, but on clusters obtained at different values of $p = p_c$,0.8, and 0.9. For the intermediate value $E \sim -1.50$, all curves have a peak at values $\rho \gtrsim 10^{-4}$, which corresponds to delocalized states. The width of the distribution is strongly dependent on p, but shows a much weaker dependency on k. It is very broad at $p = p_c$, indicating that not all sites are sufficiently visited by the particle, but the peak at $\rho \gtrsim 10^{-4}$ becomes sharper and sharper as p increases. It is also important to recall that the variation of the height of the peaks for different p is a consequence of the change in the fraction of sites with different degree as p increases.

To complete the local analysis, Fig. 9 illustrates the distribution of $\log_{10}[\rho_E(\vec{r})]$ for different values of E for a cluster at p_c. The general aspects indicated in the previous discussion can be seen in the distribution. For the band edge state corresponding to $E = -3.065$, we notice that $\rho_E(\vec{r})$ has a peak localized on sites with $k = 4$, but with significant contributions from neighboring sites with $k = 1,2$, and 3.

VI. CONCLUSIONS

We carried out an exhaustive study on the properties of $P_k(E)$ as a function of k and E. Our investigation was based both on analytical results and the numerical evaluation of $P_k(E)$ for different types of regular chains, the Apollonian network, and percolation clusters. Results for the distribution $\Pi_k[\rho_E(\vec{r})]$ on Gaussian percolation clusters have also been reported.

We have shown that $P_k(E)$ provides useful information about the energy value of the wave function that should be selected when one aims to enhance the quantum probability on sites with a specific degree. This knowledge may have practical importance, for instance, in the field of quantum information, where we know that information is generated, processed, and stored locally on quantum nodes [38], or in Josephson photonic

structures, where it is possible to make an analogy between the behavior of quantum particles and wave propagation, in which the frequency response can be controlled by tuning a magnetic field [39].

We obtained an analytical result valid for bipartite lattices of class A, where any site in the set S_1 (S_2) has not only the same degree k_1 (k_2) but also the same number of neighbors inside and outside the primitive unit cell where it is located. Under these restrictions, the product of k_i with the number of sites with degree k_i is the same for $i = 1,2$, and the probability $P_k(E \neq 0)$ of finding the particle with energy E on the sites of the sets S_1 and S_2 is independent of $E \neq 0$. We notice that the unit cell of the lattice in Fig. 1(c) does not meet the condition stated above. Indeed, in a unit cell the set S_1 has three sites with $k = 2$, two of which with $k_{1,I} = 2$ and $k_{1,E} = 0$, while the third $k_1 = 2$ site has $k_{1,I} = 1$ and $k_{1,E} = 1$. A similar result is obtained for the sites of the set S_2. Despite the fact that the demonstration of our result does not strictly apply to this lattice, our numerical results indicate that $P_k(E)$ does not depend on E. We conjecture that it may be possible to find another proof for the main result of the theorem that does not require the use of the structure of the unit cell.

For all nonhomogeneous investigated sets, the dependency of $P_k(E)$ on k and E indicates that this function has a general tendency to increase (decrease) with $|E|$ for large (small) values of k. This feature, which we showed to be exact for some decorated linear chains, has a universal character related to a basic aspect of the quantum interaction. The local analysis based on $\Pi_k[\rho_E(\vec{r})]$, which was carried out for Gaussian percolation clusters, helped clarifying the roles played by sites with different degrees on this general property of $P_k(E)$. For instance, the dominant role of $k = 4$ sites for states with E close to the band edge, highlighted by the behavior of $\Pi_k[\rho_E(\vec{r})]$, supports the effect of hybridization of the localized orbital in the denser regions, since the bandwidth is proportional to the average lattice connectivity. On the other hand, the opposite effect, namely, a larger contribution to $P_k(E)$ from sites with small k when the eigenstates are closer to the band center, is not so clear. Here, $\Pi_k[\rho_E(\vec{r})]$ shows that less localized states are spread over many sites, quite independently of their degree.

In conclusion, the function $P_k(E)$ can be easily evaluated and presents important features that are robust with respect to changes in the lattice structure and site degree, but it is not directly related to the extended or localized character of the wave function. For instance, we notice that all states of the semiregular chain in Fig. 1 are extended, which is not true for the other structures. This is why it was not possible to identify a connection between $P_k(E)$ and fine structure of wave functions like topological irregularities, or the localization of eigenstates on $k = 1$ sites or dangling bond, which also depends on its energy. The same is valid for the absence of a connection between $P_k(E)$ and other physical systems like classical random walks that are related to transport processes through diffusion [40–42]. On the other hand, the distribution $\Pi_k[\rho_E(\vec{r})]$, which shows variations with respect to p, k, and E, keeps some information on localization properties. However, the quantum conductivity with a universal character does not have a simple relation.

ACKNOWLEDGMENTS

The authors acknowledge financial support from the Brazilian agency Conselho Nacional de Desenvolvimento Científico e Tecnológico (CNPq), the Brazilian agency Fundação de Amparo à Pesquisa do Estado da Bahia (FAPESB) (Grant No. PRONEX 0006/2009), the European Research Council (Advanced Grant No. 319968-FlowCCS), and the Portuguese Foundation for Science and Technology (Contracts No. IF/00255/2013, No. UID/FIS/00618/2013, and No. EXCL/FIS-NAN/0083/2012). A.M.C.S., R.F.S.A., and H.J.H. benefitted from the support of the Instituto Nacional de Ciência e Tecnologia para Sistemas Complexos, Brazil.

APPENDIX

Here we show that, for any bipartite lattice, the quantum probability of finding a particle in any of the two subsets of sites into which the lattice is divided does not depend on the energy of the quantum state. Moreover, if 1 and 2 indicate these subsets, we obtain that $P_1(E) = P_2(E) = 1/2$.

Let us first introduce some of the spectral properties of bipartite graphs (see, e.g., [43,44]). A bipartite graph can be divided into two subsets V_1 and V_2, with N_1 and N_2 vertices, respectively, so that links connect only sites of V_1 with sites of V_2, where $N = N_1 + N_2$. In the basis $(|1\rangle_{V_1}, |2\rangle_{V_1} .. |N_1\rangle_{V_1}, |1\rangle_{V_2}, |2\rangle_{V_2} .. |N_2\rangle_{V_2})$ a state can be written as

$$|\Phi\rangle = \sum_i^{N_1} \phi_i |i\rangle_{V_1} + \sum_i^{N_2} \psi_i |i\rangle_{V_2} \tag{A1}$$

and the Hamiltonian is

$$\mathcal{H} = \begin{pmatrix} \hat{0}_{N_1,N_1} & \hat{H}' \\ \hat{H} & \hat{0}_{N_2,N_2} \end{pmatrix} \tag{A2}$$

where $\hat{0}_{n,n}$ is a matrix of size $n \times n$ the entries of which are all zeros, while $\hat{H}$ is a rectangular matrix of size $N_1 \times N_2$ where the element $\hat{H}_{i,j} = 1$ if the site $|i\rangle_{V_1}$ is connected to the site $|i\rangle_{V_2}$ and $\hat{H}_{i,j} = 0$ otherwise. The matrix $\hat{H}'$ of size $N_2 \times N_1$ is the transpose of the matrix $\hat{H}$. The coefficients ϕ_i^E and ψ_i^E of the eigenstate $|\Psi^E\rangle$ of energy E satisfy the equations

$$\hat{H}\vec{\phi}^E = E\vec{\psi}^E, \quad \hat{H}'\vec{\psi}^E = E\vec{\phi}^E, \tag{A3}$$

where we introduced the vectors $\vec{\phi} = (\phi_1^E, \ldots \phi_{N_1}^E)$ and $\vec{\psi} = (\psi_1^E, \ldots \psi_{N_2}^E)$.

The eigenstates $|\Psi^E\rangle$ of $\mathcal{H}$, with $E \neq 0$, can be obtained as follows: $\vec{\phi}^E$ has to be an eigenvector of the $N_1 \times N_1$ matrix $\hat{H}'\hat{H}$ with eigenvalue $\lambda > 0$. For each eigenvector $\vec{\phi}^E$, we have two solutions $|\Psi^E\rangle$ corresponding to $E = \pm\sqrt{\lambda}$ and $\vec{\psi}^E = \pm\sqrt{\lambda}^{-1}\hat{H}\vec{\phi}^E$ ($\vec{\psi}^E$ is an eigenvector of the $N_2 \times N_2$ matrix $\hat{H}\hat{H}'$, $\lambda\vec{\psi}_E = \hat{H}\hat{H}'\vec{\psi}^E$).

On the other hand, the eigenvectors of $\mathcal{H}$ with $E = 0$ have the form $\vec{\phi}^E = \vec{\phi}^0$ and $\vec{\psi}^E = \vec{0}_{N_2}$ or $\vec{\phi}^E = \vec{0}_{N_1}$ and $\vec{\psi}^E = \vec{\psi}^0$ where $\vec{\phi}_0$ ($\vec{\psi}_0$) belongs to the kernel of $\hat{H}'\hat{H}$ ($\hat{H}\hat{H}'$) and $\vec{0}_N$ is the null vector of size N.

Since all the eigenvalues λ of $\hat{H}'\hat{H}$ and $\hat{H}\hat{H}'$ are nonnegative, we obtain the full description of the spectrum. If M is the number of the nonzero eigenvalues of $\hat{H}'\hat{H}$ (M is

also the number of nonzero eigenvalues of $\hat{H}\hat{H}'$), there are $2M$ nonzero eigenvalues of $\mathcal{H}$ (M with $E=\sqrt{\lambda}$ and M with $E=-\sqrt{\lambda}$), and then we have N_1-M null eigenvalues of the form $\vec{\phi}^E=\vec{\phi}^0$ and $\vec{\psi}^E=\vec{0}_{N_2}$ and N_2-M null eigenvalues of the form $\vec{\phi}^E=\vec{0}_{N_1}$ and $\vec{\psi}^E=\vec{\psi}^0$.

For the eigenstate $|\Psi^E\rangle$ the probability of finding the particle in the set V_1 is

$$P_1(E)=\frac{(\vec{\phi}^E\cdot\vec{\phi}^E)}{(\vec{\phi}^E\cdot\vec{\phi}^E)+(\vec{\psi}^E\cdot\vec{\psi}^E)}, \tag{A4}$$

where $(\,\cdot\,)$ denotes the scalar product. If we introduce the expression for $\vec{\psi}^E$ when $E\neq 0$ we get

$$\begin{aligned}P_1(E)&=\frac{(\vec{\phi}^E\cdot\vec{\phi}^E)}{(\vec{\phi}^E\cdot\vec{\phi}^E)+(\pm\sqrt{\lambda}^{-1}\hat{H}\vec{\phi}^E\cdot\pm\sqrt{\lambda}^{-1}\hat{H}\vec{\phi}^E)}\\&=\frac{(\vec{\phi}^E\cdot\vec{\phi}^E)}{(\vec{\phi}^E\cdot\vec{\phi}^E)+\lambda^{-1}(\vec{\phi}^E\cdot\hat{H}'\hat{H}\vec{\phi}^E)}\\&=\frac{(\vec{\phi}^E\cdot\vec{\phi}^E)}{(\vec{\phi}^E\cdot\vec{\phi}^E)+(\vec{\phi}^E\cdot\vec{\phi}^E)}=\frac{1}{2}.\end{aligned} \tag{A5}$$

Clearly we get the same probability $1/2$ of finding a particle in V_2. Taking into account that the number of eigenstates with $E=0$ which belong to V_1 and V_2 are N_1-M and N_2-M, respectively, we have that at $E=0$ the probabilities of finding a particle in V_1 and in V_2 are $P_1(0)=(N_1-M)/(N-2M)$ and $P_2(0)=(N_2-M)/(N-2M)$.

If we are considering a bipartite graph where all the vertices in V_1 have degree k_1 and all the vertices in V_2 have degree k_2, it is clear that, for all eigenvalues $E\neq 0$, the probabilities of having degree k_1 and k_2 are $P_{k_1}(E)=P_{k_2}(E)=1/2$. Moreover, at $E=0$ since $N_1k_1=N_2k_2$ and $N_1+N_2=N$, we have

$$\begin{aligned}P_{k_1}(0)&=\frac{Nk_2/(k_1+k_2)-M}{N_M},\quad\text{and}\\P_{k_2}(0)&=\frac{Nk_1/(k_1+k_2)-M}{N_M},\end{aligned} \tag{A6}$$

where the integer M depends on the particular biregular graph that we are considering. We notice that, if $k_1<k_2$, $P_{k_1}(0)>P_{k_2}(0)$ so that, also for biregular structures at small $|E|$, there is a larger probability to find the particle in the sites with smaller degree, as has been observed in numerical simulations, in general. However, due to the peculiarity of the graph this is only evident at $E=0$.

[1] N. W. Ashcroft and N. D. Mermin, *Solid State Physics*, 1st ed. (Harcourt, Orlando, 1976).
[2] P. W. Anderson, Phys. Rev. **109**, 1492 (1958).
[3] F. Evers and A. D. Mirlin, Rev. Mod. Phys. **80**, 1355 (2008)
[4] I. J. Farkas, I. Derenyi, A.-L. Barabasi, and T. Vicsek, Phys. Rev. E **64**, 026704 (2001).
[5] L. Jahnke, J. W. Kantelhardt, R. Berkovits, and S. Havlin, Phys. Rev. Lett. **101**, 175702 (2008).
[6] O. Giraud, B. Georgeot, and D. L. Shepelyansky, Phys. Rev. E **80**, 026107 (2009).
[7] M. Schreiber and H. Grussbach, Phys. Rev. Lett. **76**, 1687 (1996).
[8] F. A. B. F. de Moura and M. L. Lyra, Phys. Rev. Lett. **81**, 3735 (1998).
[9] M. F. Islam and H. Nakanishi, Eur. Phys. J. B **68**, 123 (2009).
[10] Z. Darazs and T. Kiss, J. Phys. A **46**, 375305 (2013).
[11] C. M. Chandrashekar and Th. Busch, Scientific Reports **4**, 6583 (2014).
[12] A. M. S. Macêdo, M. C. dos Santos, M. D. Coutinho-Filho, and C. A. Macêdo, Phys. Rev. Lett. **74**, 1851 (1995).
[13] S. R. Broadbent and J. M. Hammersley, Proc. Cambridge Philos. Soc. **53**, 629 (1957).
[14] D. Stauffer and A. Aharony, *Introduction to Percolation Theory*, 2nd ed. (Taylor & Francis, London, 1994).
[15] N. A. M. Araujo and H. J. Herrmann, Phys. Rev. Lett. **105**, 035701 (2010).
[16] J. S. Andrade, Jr., H. J. Herrmann, R. F. S. Andrade, and L. R. da Silva, Phys. Rev. Lett. **94**, 018702 (2005).
[17] A. L. Cardoso, R. F. S. Andrade, and A. M. C. Souza, Phys. Rev. B **78**, 214202 (2008).
[18] I. N. de Oliveira, F. A. B. F. de Moura, M. L. Lyra, J. S. Andrade, Jr., and E. L. Albuquerque, Phys. Rev. E **79**, 016104 (2009).
[19] A. B. Harris, Phys. Rev. B **29**, 2519 (1984).
[20] T. Odagaki and K. C. Chang, Phys. Rev. B **30**, 1612(R) (1984).
[21] I. Chang, Z. Lev, A. B. Harris, J. Adler, and A. Aharony, Phys. Rev. Lett. **74**, 2094 (1995).
[22] J. W. Kantelhardt, A. Bunde, and L. Schweitzer, Phys. Rev. Lett. **81**, 4907 (1998).
[23] G. Schubert and H. Fehske, Phys. Rev. B **77**, 245130 (2008).
[24] M. F. Islam and H. Nakanishi, Phys. Rev. E **77**, 061109 (2008).
[25] L. Gong and P. Tong, Phys. Rev. B **80**, 174205 (2009).
[26] S. S. de Albuquerque, F. A. B. F. de Moura, and M. L. Lyra, J. Phys.: Condens. Matter **24**, 205401 (2012).
[27] B. S. Dillona and H. Nakanishi, Eur. Phys. J. B **87**, 286 (2014).
[28] F. Harari, *Graph Theory* (Addison-Wesley, Reading, MA, 1969).
[29] R. Albert and A. L. Barabási, Rev. Mod. Phys. **74**, 47 (2002).
[30] M. Newman, *Networks, An Introduction* (Oxford University, Oxford, 2010).
[31] M. Cvetkovic, M. Doob, and H. Sachs, *Spectra of Graphs. Theory and Application* (Academic, New York, 1980).
[32] P. Van Meighem, *Graph Spectra for Complex Networks* (Cambridge University, Cambridge, England, 2011).
[33] J. M. G. Cowie, *Polymers: Chemistry and Physics of Modern Material* (Blackie, Glasgow, 1991).
[34] P. C. Painter, and M. M. Coleman, *Fundamentals of Polymer Science: An Introductory Text* (Technomic, Lancaster, PA, 1997).
[35] R. F. S. Andrade and J. G. V. Miranda, Physica A **356**, 1 (2005).
[36] X.-P. Xu, W. Li, and F. Liu, Phys. Rev. E **78**, 052103 (2008).
[37] A. M. C. Souza and R. F. S. Andrade, J. Phys. A **46**, 145102 (2013).
[38] G. M. A. Almeida and A. M. C. Souza, Phys. Rev. A **87**, 033804 (2013).

[39] V. A. Yampolkii, S. Savelev, O. V. Usatenko, S. S. Melnik, F. V. Kusmartsev, A. A. Krokhin, and F. Nori, Phys. Rev. B **75**, 014527 (2007).

[40] R. Burioni, D. Cassi, I. Meccoli, and S. Regina, Phys. Rev. B **61**, 8614 (2000).

[41] R. Burioni, D. Cassi, M. Rasetti, P. Sodano, and A. Vezzani, J. Phys. B **34**, 4697 (2001).

[42] P. Buonsante, R. Burioni, and D. Cassi, Phys. Rev. B **65**, 054202 (2002).

[43] A. E. Brouwer and W. H. Haemers, *Spectra of Graphs* (Springer-Verlag, New York, 2012).

[44] A. S. Asratian, T. M. J. Denley, and R. Hggkvist, *Bipartite Graphs and Their Applications* (Cambridge University, Cambridge, England, 1998).